Dual-responsive “smart” window and visually attractive coating based on a diarylethene photochromic dye

Research Article Vol. 58, No. 36 / 20 December 2019 / Applied Optics 9823

applied optics

Dual-responsive "smart" window and visually attractive coating based on a diarylethene photochromic dye

Gilles H. Timmermans,[1,†] Bartholomeus W. H. Saes,[2,†] and Michael G. Debije[1,*]

[1]Stimuli-responsive Functional Materials and Devices, Chemical Engineering & Chemistry, Eindhoven University of Technology, 5600 MB Eindhoven, The Netherlands
[2]Molecular Materials and Nanosystems, Chemical Engineering & Chemistry, Eindhoven University of Technology, 5600 MB Eindhoven, The Netherlands
*Corresponding author: m.g.debije@tue.nl

Received 15 September 2019; revised 30 October 2019; accepted 4 November 2019; posted 6 November 2019 (Doc. ID 378027); published 11 December 2019

Controlling the intensity and manipulating the spectral composition of sunlight are critical for many devices including "smart" windows, greenhouses, and photomicroreactors, but these are also important in more decorative applications. Here, we use a diarylethene dye incorporated in a liquid crystal host to create a dual-responsive "smart" window regulated both by an electrical trigger and by specific wavelengths of light. By incorporating the same diarylethene dye in a polymerizable host and using inkjet printing, coatings can be made with complete freedom in the applied pattern design, although the electrical response is lost. The color change of the diarylethene dye can be controlled in simulated sunlight by concurrent light exposure from an LED source, allowing a manual override for outdoor use. Photoluminescence of the closed isomer of the diarylethene from the light guide edges could be used for lighting or electricity generation in a luminescent solar concentrator architecture.

https://doi.org/10.1364/AO.58.009823

1. INTRODUCTION

Currently, buildings demand around 40% of global energy production. [1,2] Around half of this consumed energy is used for heating, cooling, and ventilation, which could be greatly reduced through better control of the incoming sunlight [2]. One way to control the incoming light is by using "smart" windows, which can reversibly change their optical properties [3] in response to external stimuli including electricity [4–6], temperature [7–9], and light [10–12].

Smart windows can be further improved by designing them to generate electricity themselves. One way to generate electricity in smart windows is by using the luminescent solar concentrator (LSC) concept [13,14]. An LSC is a light guide made from glass or polymer coated with or containing a luminescent dye. Part of the light that penetrates the light guide surface is absorbed and re-emitted at a longer wavelength by the luminescent dye. Due to the higher refractive index of the light guide compared with the surrounding air, a significant fraction of the light emitted by the dye is trapped in the device by total internal reflection and guided to the edges of the plate where photovoltaic cells (PVs) can be attached for light-to-electricity conversion. The majority of LSC devices have been proposed for use as electricity generators from solar light, but applications have also been proposed for using the emission light for daylighting, [15] greenhouses [6], and even the production of fine chemicals [16,17].

One way to help in the introduction of smart windows into the built environment and reduce manufacturing costs is by using "smart" coatings. Coatings are easier to scale up and produce, especially when the need for electrodes is removed. Inkjet printing such coatings allows for creative patterns to be produced that can be made more visually attractive.

In this paper, we demonstrate the concept of a dual electrically switchable and photoswitchable smart window, which can be used to generate electricity. Additionally, an exclusively photoswitchable system was fabricated by inkjet printing, which could ease the application of energy-generating smart windows in the urban setting via its visually pleasing aesthetics. To our knowledge, no other light-switchable, color-changing LSC coatings have been reported in literature. The key component is the photochromic dye (see Fig. 1), which, due to its small conformational change upon isomerization, enables switching between the colored and transparent states when embedded in a polymeric host [18,19]. Photochromic diarylethenes have previously found application in fields including optical data

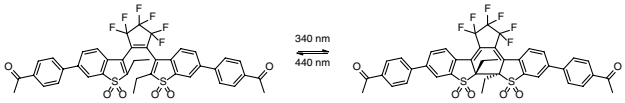

Fig. 1. Molecular structures of the photochromic diarylethene dye in its open, nonfluorescent form (left) and its closed, fluorescent form (right).

storage [20,21], thermosensors [22], display materials [23], and in biotechnology [24]. However, diarylethenes with fluorescent quantum yields above 0.7 (required for LSC applications) are uncommon [22,25–28].

2. RESULTS

1,2-Bis(2-ethyl-6-(4-acetylphenyl)-1-benzothiophen-1,1-dioxide-3-yl)perfluorocyclopentene (hereafter labeled the "diarylethene dye"; see Fig. 1) was chosen as the photoswitchable dye. The choice for this dye is mainly based on its high fluorescence quantum yield (Φ_F) in the ring-closed isomer (in 1,4-dioxane, $\Phi_F = 0.87$) [25]. Diarylethene dyes with *S*, *S*-dioxidized benzothiophene heterocycles have a significantly increased Φ_F compared with their thiophene heterocycle appended counterparts. Extension of the conjugation raises the Φ_F from 0.22 to ≈ 0.8: this is why the molecule features acetophenone rings in conjugation with the benzothiophene heterocycles. In addition, from a series of molecules where the length of linear alkyl substituents on the reactive carbons of similar diarylethenes is varied from methyl up to *n*-butyl in order to increase Φ_F, substituents longer than methyl on the benzothiophene 2-position are most effective [29]. However, the introduction of ethyl alkyl chains may diminish the fatigue resistance of diarylethenes compared with their methyl substituted counterparts; for proof of principle, we valued the increased Φ_F over the increased fatigue resistance.

0.25 wt. % of the diarylethene dye was dissolved in E7, a commonly used liquid crystal (LC) [4,30] mixture, which is nematic at room temperature and used to fill a 5×5 cm^2 indium tin oxide (ITO)-coated, planar-aligned glass cell with a 20 μm cell gap. In this setup, dual electrical-optical switching behavior could be tested. The order parameter (*S*) of the dye within this system was determined by comparing the absorption of light polarized parallel (A_{par}) and perpendicular (A_{per}) to the alignment of the dye with the following equation:

$$S = \frac{A_{par} - A_{per}}{A_{par} + 2A_{per}}.$$

These measurements resulted in a relatively high-order parameter of $S = 0.53$, comparable to the order parameter of the better-aligning dyes used in previous studies [31,32].

The center of the planar cell was then covered with an opaque photomask in the shape of a cross, and the device was exposed for 2 h to light from a 440 nm LED. Upon removal of the photomask, a dark yellow cross corresponding to the unexposed areas was visible on a mostly transparent background from the exposed regions, as can be seen in Fig. 2(a). Figure 2(c) shows schematically that light is able to pass the sample in the exposed areas where the dye has undergone a ring opening to the transparent state while the light is absorbed at the unexposed areas.

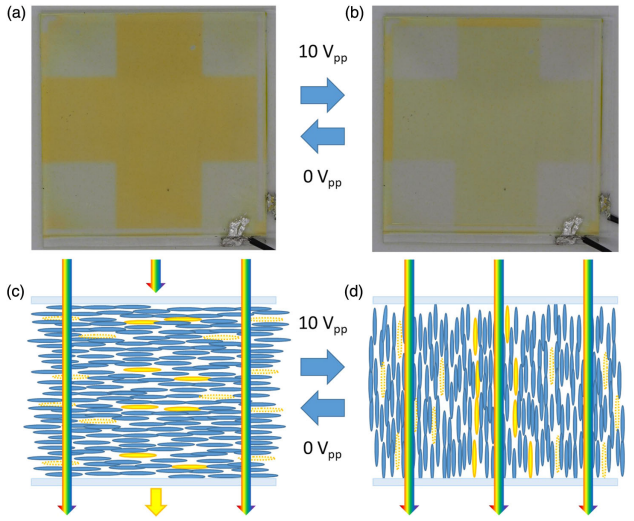

Fig. 2. (a) Photograph of a 20 μm cell of 0.25 wt. % diarylethene dye in the host liquid crystal E7 exposed for 2 h to 440 nm light through a cross-shaped mask. (b) The same sample with 10 V_{pp} at 100 Hz applied. (c) Schematic representation of the alignment of the LCs and the dye in both open and closed forms in rest state (0 V_{pp}). (d) Schematic representation of the alignment of the LCs and the dye in both open and closed states in the homeotropic orientation (10 V_{pp}).

By application of a small AC field (i.e., 10 V_{pp} at 100 Hz), the LC (and hence the diarylethene dye) could be reoriented into a homeotropic state within a second [see Fig. 2(b)]. Due to the dichroism of the dye, the absorption is much reduced in the regions with homeotropic orientation compared with the planar (rest) state, resulting in the dark yellow areas becoming more transparent while the background became even clearer. Figure 2(d) shows the realignment of the LCs and the dye, resulting in a nonabsorbing state across the sample allowing more light to pass through the device. Removal of the potential allows the LCs to return to their initial orientation within seconds. These multiple visual effects are not normally possible in "smart" windows using static fluorescent dichroic dyes.

The absorption spectra of the exposed and unexposed regions of the sample are shown in Fig. 3. The unexposed area covered by the mask retained its initial absorbance, indicating that no isomerization has occurred, in contrast to the region exposed to the LED for 2 h, where a decrease of the absorbance peak from 0.19 to 0.08 was observed. The LC (and hence the diarylethene dye) reoriented reversibly upon application of a potential across the cell to align homeotropically, resulting in a drop in the measured absorption of the exposed areas to only 0.04, while the absorption of the masked area reduced to 0.08. In the future, to reduce the switching times without affecting the fluorescent quantum yield, it may be possible to modify the dye to have an increased thermal relaxation.

By incorporating the diarylethene dye in a solution, inkjet printing allows for the construction of intricate, light-sensitive art, making the system more visually pleasing to the observer. For example, Fig. 4(a) displays a sample printed in the shape of a flower, with the center yellow region containing the diarylethene dye and the outer red region containing BASF Lumogen F Red 305, a common dye used in LSC studies. [16,33–36] The sample, containing 0.45 wt. % of diarylethene dye in a binder,

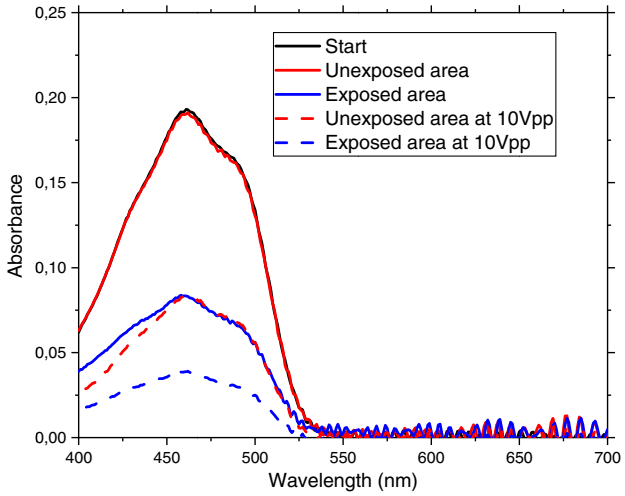

Fig. 3. Absorption spectra of the exposed (blue) and unexposed (red) regions of the masked cell containing 0.25 wt. % diarylethene dye in E7 at rest (solid lines) and under an applied field of 10 V_{pp} at 100 Hz (dotted lines). For references to color, the reader is requested to refer to the online version of the paper.

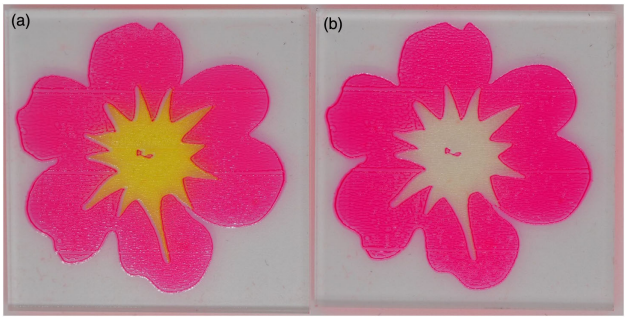

Fig. 4. Examples of an inkjet-printed pattern containing diarylethene dye (yellow) and Lumogen F Red 305 (red): (a) a flower; (b) a flower after switching to the transparent state (2 h of 440 nm light). For references to color, the reader is requested to refer to the online version of the paper.

was printed onto $5 \times 5 \times 0.5$ cm^3 polymethylmethacrylate (PMMA) plates. The printed layer was subsequently photopolymerized under nitrogen with a 365 nm LED to form a solid film. During the polymerization, photocyclization of the diarylethene took place accompanied with the enhancement of the absorption band at around 455 nm. Figure 4(b) shows the same flower after switching to the transparent state (2 h of 440 nm light), resulting in a fading of the color of the flower center, with only the red petal color remaining. This allows for decorative designs that could be used for advertisement purposes where part of the message can be reversibly displayed.

To study the switching speed and light being emitted from the edges of the light guide, the diarylethene dye was printed to fully cover the 5×5 cm^2 surface of a PMMA plate. After photopolymerization (and photocyclization of the diarylethene) of the binder, the sample was exposed to light from a 440 nm LED at 22 mW/cm^2, causing a photoinduced cycloreversion and gradual reduction of the absorption peak center at 455 nm

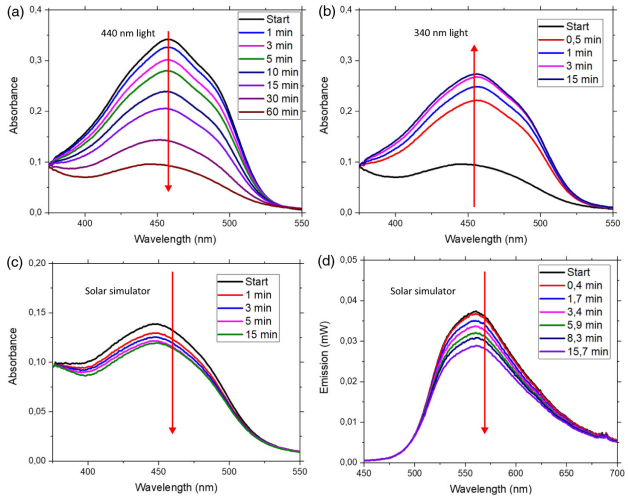

Fig. 5. Absorption spectra of the coating containing the diarylethene dye on a PMMA light guide. (a) During exposure with 440 nm light. (b) During subsequent exposure with 340 nm light. (c) During subsequent exposure with solar simulator AM 1.5 illumination. (d) Edge emission spectra of the diarylethene dye on a PMMA light guide during exposure with solar simulator AM 1.5 illumination.

[see Fig. 5(a)], changing the film color from yellow to essentially colorless over an hour of exposure. To regenerate the absorption peak and device color, the sample was exposed to 340 nm light from an LED at 1.5 mW/cm^2, reaching the photostationary state (PSS) within 3 min. Already more than 80% of the maximum absorption at 455 nm of the pristine coating was recovered within the first 30 s [Fig. 5(b)]. The PSS was also monitored under a solar simulator. This resulted in a 14% decrease of the absorption from the initial fluorescent state [see Fig. 5(c)]. The dye reached this PSS in less than 15 min of exposure to the solar simulator, which generates a continuous spectrum, simultaneously exciting both the open and closed isomers of the diarylethene.

The fluorescent light emitted by the dye is largely retained in the high-refractive-index PMMA light guide by total internal reflection, and exits the material primarily through the edges of the plate. The fluorescent light emitted from one edge of the light guide during exposure to the solar simulator was captured with an integrating sphere and spectrally resolved [see Fig. 5(d)]. The intensity of the emitted light decreases in time, concurrent with the decrease of absorption at 455 nm. The internal optical efficiency [37] (photons emitted at the edges of the device per photons absorbed by the device) of the initial closed isomer, high absorbance state was calculated using

$$\eta_{\text{int}} = \frac{\text{photons emitted}}{\text{photons absorbed}}$$

$$= \frac{\int_{\text{emission}} P_{\text{out}}(\lambda_{\text{em}}) \frac{\lambda_{\text{em}}}{hc} d\lambda_{\text{em}}}{\int_{\text{absorption}} P_{\text{in}}(\lambda_{\text{abs}}) \frac{\lambda_{\text{abs}}}{hc} A(\lambda) d\lambda_{\text{abs}}} * 100\%,$$

where $P_{\text{out}}(\lambda_{\text{em}})$ is the emission of all four edges over the wavelength range (in watts). Because only 1 edge could be physically measured, total output was approximated by multiplying the

single measurement by four. $P_{in}(\lambda_{abs})$ is the incoming light spectra from the solar simulator (in watts), $A(\lambda)$ is the absorption of the sample (in %), λ is the wavelength range over which the summation is made, h is Planck's constant, and c is the speed of light. For the active wavelength range (absorption 350–800 nm, emission 450–700 nm), the calculated internal optical efficiency was $\eta_{int} = 40\%$ (10% for a single edge).

Illumination of the sample with exclusively 440 nm light initially resulted in a high emission, which dropped by more than 50% within 30 min due to the ring opening reaction to the transparent, nonfluorescent state (see Fig. 6). Illumination with 340 nm light resulted in only negligible emission (see Fig. 7) as the closed isomer shows practically no absorption at this wavelength.

For future applications, it would be desirable to control the color change in the LSC device in an outdoor environment, where constant solar light is illuminating the device. This control is simulated by illumination with a solar simulator until the PSS is reached, followed by supplementing the solar simulator with an additional 440 nm LED light source to alter the PSS [this sequence is illustrated as an inset in Fig. 6(a)] and to drive the device towards its open, transparent isomer. The addition of the 440 nm LED increases the light intensity on the sample, resulting in an increase of emission between 500 and 700 nm [see Fig. 6(a)]. After the initial increase, the transition towards the open and transparent isomer decreases the emission [see Fig. 6(b)], indicating that the PSS and the accompanying color and fluorescence states can be tuned to desired levels.

To restore the original state, illumination with the 440 nm LED was ceased, allowing the sample to return to the PSS under simulated solar illumination. This was followed by illumination with a 340 nm LED, driving the dye towards its closed fluorescent state, resulting in increased emission. The principle of this tuning is shown in Fig. 7; however, the changes in the emission are minor, resulting from the large difference in intensity between the 340 nm LED and the solar simulator (1.5 mW/cm^2 versus 22.5 mW/cm^2, respectively) and competitive absorption of the binder, allowing for only a minor shift in the PSS of the device.

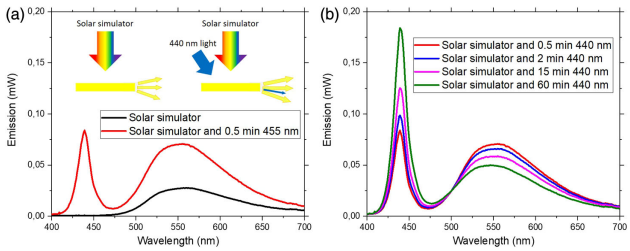

Fig. 6. Edge emissions of the diarylethene dye film (a) upon initial illumination by a solar simulator (black line) and with additional 440 nm LED (red line) illumination (inset, schematic of the setup) followed by (b) time evolution of the edge emission during continuous exposure to solar simulator light with additional 440 nm light illumination. The short wavelength peak in the spectra is the result of LED light scattered to and escaping the edge of the light guide; the peak increases over time as the sample becomes more transparent to these wavelengths over time. For references to color, the reader is requested to refer to the online version of the paper.

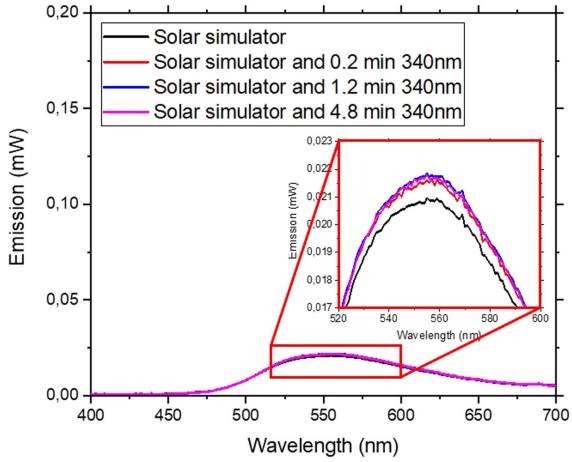

Fig. 7. Time evolution of the edge emission under illumination of the AM 1.5 G solar spectrum. Inset, enlargement of the emission peak.

Photoswitching is not fully reversible for the coating or the LC matrix: degradation could play a role in this as well as other mechanisms such as crystallization and dye reorientation. Degradation mechanisms of this class of dyes have been extensively studied in the literature [38–42]: the dye host has a significant impact on stability [43]. Overall improvements in the dye lifetime will be necessary before it may be widely used in applications but extended switching capabilities have already been demonstrated [21].

For future development and commercialization, the library of switchable fluorescent molecules should be extended to exhibit a wider variety of colors. Fortunately, the color of these molecules can be easily altered, suggesting deployment in the built environment from the aesthetic standpoint could be possible with smart windows as advertisement banners, where parts of the message could be reversibly manipulated. Finally, the color switching could find application in the LSC-photomicroreactor concept, [16,44] allowing various reactions to be catalyzed from solar light by simply switching the color state of the embedded diarylethene.

3. EXPERIMENT

Diarylethene dye was synthesized according to procedures found in the literature [26]. Lumogen F Red 305 (Red 305) [33] was purchased from BASF SE, and the nematic LC mix E7 was purchased from Merck KGaA. A proprietary solution was used for the inkjet printing. Samples were printed on 50 × 50 × 5 mm^3 PMMA substrates (Plano Plastics). Inkjet printing was performed on a Dimatix DMP-2831 printer equipped with a DMC11610 printhead (10 pl). Polymerization of the ink was performed with a Thorlabs M365LP1 LED under N_2 at a dose rate of 35 mW/cm^2. Custom-made ITO coated cells (about 50 × 50 mm^2 switching area, coated with planar-aligned polyimide, 20 μm spacing) were purchased from LC-Tec Displays AB.

UV–visible spectra were measured on a PerkinElmer Lambda 750 with a 150 mm integrating sphere. Edge emissions were measured using a Labsphere SLMS 1050 integrating sphere

connected to an International Light RPS900 diode array detector. Simulated solar illumination was provided by a 300 W Lot-Oriel solar simulator equipped with filters to emulate the AM 1.5 solar spectrum. Additional illumination was provided with Thorlabs LEDs of 340 nm (M340L4) and 440 nm (M455L3) with collimation adapters placed approximately 19 cm above the sample at 700 mA. A function generator (Agilent 33220A) was used to apply a 10 V_{pp}, 100 Hz sine wave.

4. CONCLUSION

In this work, we have shown a diarylethene-based electrically switchable and photoswitchable "smart" window with a potential for electricity generation. Additionally, using inkjet printing, diarylethene-based coatings could be created allowing for more visually appealing designs. Printing these coatings results in the loss of the electrical switching response but will also lower the manufacturing costs as electrodes are no longer needed. The coating is capable of switching its coloration when exposed to light from LEDs as well as solar-simulated light; the fluorescence escaping the edge of the underlying light guide is affected by the switching state of the dye. The color change is reversible, although the stability at this time must be improved before real applications can be considered. A "manual override" for the color change under the solar simulator was created by adding additional light from an LED. If desired, it is possible to maintain the color of the dye to a significant degree, even under fully simulated sunlight. These systems could help reduce energy consumption in buildings by being employed as smart windows or signage, for example.

Funding. TKI (PPS Smart Materials for Greenhouses).

Acknowledgment. MD and GT acknowledge the support of the TKI PPS Smart Materials for Greenhouses program for its support of this work. We would like to thank M. Irie and M. Morimoto for helpful advice on the dye synthesis and for providing a precursor to the synthesized diarylethene dye. We would like to thank R. A. J. Janssen and S. Fredrich for their comments and suggestions on the paper.

Disclosures. The authors declare no conflicts of interest.

[†]These authors contributed equally to this work.

REFERENCES

1. A. M. Omer, "Energy, environment and sustainable development," Renewable Sustainable Energy Rev. **12**, 2265–2300 (2008).
2. Y. Ke, C. Zhou, Y. Zhou, S. Wang, S. H. Chan, and Y. Long, "Emerging thermal-responsive materials and integrated techniques targeting the energy-efficient smart window application," Adv. Funct. Mater. **28**, 1800113 (2018).
3. Y. Ke, J. Chen, G. Lin, S. Wang, Y. Zhou, J. Yin, P. S. Lee, and Y. Long, "Smart windows: electro-, thermo-, mechano-, photochromics, and beyond," Adv. Energy Mater. **9**, 1902066 (2019).
4. H. Khandelwal, R. C. G. M. Loonen, J. L. M. Hensen, M. G. Debije, and A. P. H. J. Schenning, "Electrically switchable polymer stabilised broadband infrared reflectors and their potential as smart windows for energy saving in buildings," Sci. Rep. **5**, 11773 (2015).
5. H. Khandelwal, M. G. Debije, T. J. White, and A. P. H. J. Schenning, "Electrically tunable infrared reflector with adjustable bandwidth broadening up to 1100 nm," J. Mater. Chem. A **4**, 6064–6069 (2016).
6. J. A. H. P. Sol, G. H. Timmermans, A. J. van Breugel, A. P. H. J. Schenning, and M. G. Debije, "Multistate luminescent solar concentrator "Smart" windows," Adv. Energy Mater. **8**, 1702922 (2018).
7. L. Wang, H. K. Bisoyi, Z. Zheng, K. G. Gutierrez-Cuevas, G. Singh, S. Kumar, T. J. Bunning, and Q. Li, "Stimuli-directed self-organized chiral superstructures for adaptive windows enabled by mesogen-functionalized graphene," Mater. Today **20**(5), 230–237 (2017).
8. E. P. A. van Heeswijk, J. J. H. Kloos, N. Grossiord, and A. P. H. J. Schenning, "Humidity-gated, temperature-responsive photonic infrared reflective broadband coatings," J. Mater. Chem. A **7**, 6113–6119 (2019).
9. H. Khandelwal, G. H. Timmermans, M. G. Debije, and A. P. H. J. Schenning, "Dual electrically and thermally responsive broadband reflectors based on polymer network stabilized chiral nematic liquid crystals: the role of crosslink density," Chem. Commun. **52**, 10109–10112 (2016).
10. J. R. Talukder, Y.-H. Lee, and S.-T. Wu, "Photo-responsive dye-doped liquid crystals for smart windows," Opt. Express **27**, 4480–4487 (2019).
11. T. J. White, R. L. Bricker, L. V. Natarajan, S. V. Serak, N. V. Tabiryan, and T. J. Bunning, "Polymer stabilization of phototunable cholesteric liquid crystals," Soft Matter **5**, 3623–3628 (2009).
12. J. R. Talukder, H.-Y. Lin, and S.-T. Wu, "Photo- and electrical-responsive liquid crystal smart dimmer for augmented reality displays," Opt. Express **27**, 18169–18179 (2019).
13. M. G. Debije and P. P. C. Verbunt, "Thirty years of luminescent solar concentrator research: solar energy for the built environment," Adv. Energy Mater. **2**, 12–35 (2012).
14. B. McKenna and R. C. Evans, "Towards efficient spectral converters through materials design for luminescent solar devices," Adv. Mater. **29**, 1606491 (2017).
15. A. A. Earp, G. B. Smith, J. Franklin, and P. D. Swift, "Optimisation of a three-colour luminescent solar concentrator daylighting system," Sol. Energy Mater. Sol. Cells **84**, 411–426 (2004).
16. D. Cambié, F. Zhao, V. Hessel, M. G. Debije, and T. Noël, "A leaf-inspired luminescent solar concentrator for energy-efficient continuous-flow photochemistry," Angew. Chem. Int. Ed. **56**, 1050–1054 (2017).
17. F. Zhao, D. Cambié, V. Hessel, M. G. Debije, and T. Noël, "Real-time reaction control for solar production of chemicals under fluctuating irradiance," Green Chem. **20**, 2459–2464 (2018).
18. M. Irie, T. Fukaminato, K. Matsuda, and S. Kobatake, "Photochromism of diarylethene molecules and crystals: memories, switches, and actuators," Chem. Rev. **114**, 12174–12277 (2014).
19. M. Morimoto, S. Kobatake, and M. Irie, "Polymorphism of 1, 2-Bis(2-methyl-5-p-methoxyphenyl-3-thienyl)perfluorocyclopentene and photochromic reactivity of the single crystals," Chem. Eur. J. **9**, 621–627 (2003).
20. M. Irie, "Diarylethenes for memories and switches," Chem. Rev. **100**, 1685–1716 (2000).
21. M. Yu, H. Wang, Y. Li, P. Zhang, S. Chen, R. Zeng, Y. Gao, and J. Chen, "Photoswitchable diarylethene-based polyurethane film for photorewritable patterning and stable information storage," J. Appl. Polym. Sci. **136**, 1–7 (2019).
22. D. Kitagawa and S. Kobatake, "Strategy for molecular design of photochromic diarylethenes having thermal functionality," Chem. Rec. **16**, 2005–2015 (2016).
23. S. Kobatake, H. Imagawa, H. Nakatani, and S. Nakashima, "The irreversible thermo-bleaching function of a photochromic diarylethene having trimethylsilyl groups," New J. Chem. **33**, 1362–1367 (2009).
24. X. Su, Y. Ji, W. Pan, S. Chen, Y.-M. Zhang, T. Lin, L. Liu, M. Li, Y. Liu, and S. X.-A. Zhang, "Pyrene spiropyran dyad: solvato-, acido- and mechanofluorochromic properties and its application in acid sensing and reversible fluorescent display," J. Mater. Chem. C **6**, 6940–6948 (2018).
25. Y. Takagi, T. Kunishi, T. Katayama, Y. Ishibashi, H. Miyasaka, M. Morimoto, and M. Irie, "Photoswitchable fluorescent diarylethene

derivatives with short alkyl chain substituents," Photochem. Photobiol. Sci. **11**, 1661–1665 (2012).
26. K. Uno, H. Niikura, M. Morimoto, Y. Ishibashi, H. Miyasaka, and M. Irie, "In situ preparation of highly fluorescent dyes upon photoirradiation," J. Am. Chem. Soc. **133**, 13558–13564 (2011).
27. M. Morimoto, Y. Takagi, K. Hioki, T. Nagasaka, H. Sotome, S. Ito, H. Miyasaka, and M. Irie, "A turn-on mode fluorescent diarylethene: solvatochromism of fluorescence," Dyes Pigm. **153**, 144–149 (2018).
28. R. Kashihara, M. Morimoto, S. Ito, H. Miyasaka, and M. Irie, "Fluorescence photoswitching of a diarylethene by irradiation with single-wavelength visible light," J. Am. Chem. Soc. **139**, 16498–16501 (2017).
29. M. Irie and M. Morimoto, "Photoswitchable turn-on mode fluorescent diarylethenes: strategies for controlling the switching response," Bull. Chem. Soc. Jpn. **91**, 237–250 (2018).
30. M. E. McConney, T. J. White, V. P. Tondiglia, L. V. Natarajan, D. Yang, and T. J. Bunning, "Dynamic high contrast reflective coloration from responsive polymer/cholesteric liquid crystal architectures," Soft Matter **8**, 318–323 (2012).
31. P. P. C. Verbunt, A. Kaiser, K. Hermans, C. W. M. Bastiaansen, D. J. Broer, and M. G. Debije, "Controlling light emission in luminescent solar concentrators through use of dye molecules aligned in a planar manner by liquid crystals," Adv. Funct. Mater. **19**, 2714–2719 (2009).
32. M. G. Debije, "Solar energy collectors with tunable transmission," Adv. Func. Mater. **20**, 1498–1502 (2010).
33. G. Seybold and G. Wagenblast, "New perylene and violanthrone dyestuffs for fluorescent collectors," Dyes Pigm. **11**, 303–317 (1989).
34. L. H. Slooff, E. E. Bende, A. R. Burgers, T. Budel, M. Pravettoni, R. P. Kenny, E. D. Dunlop, and A. Büchtemann, "A luminescent solar concentrator with 7.1% power conversion efficiency," Phys. Status Solidi RRL **2**, 257–259 (2008).
35. J. C. Goldschmidt, M. Peters, A. Bösch, H. Helmers, F. Dimroth, S. W. Glunz, and G. P. Willeke, "Increasing the efficiency of fluorescent concentrator systems," Sol. Energy Mater. Sol. Cells **93**, 176–182 (2009).
36. L. Desmet, A. J. M. Ras, D. K. G. De Boer, and M. G. Debije, "Monocrystalline silicon photovoltaic luminescent solar concentrator with 4.2% power conversion efficiency," Opt. Lett. **37**, 3087–3089 (2012).
37. C. Tummeltshammer, A. Taylor, A. J. Kenyon, and I. Papakonstantinou, "Losses in luminescent solar concentrators unveiled," Sol. Energy Mater. Sol. Cells **144**, 40–47 (2016).
38. M. Herder, B. M. Schmidt, L. Grubert, M. Pätzel, J. Schwarz, and S. Hecht, "Improving the fatigue resistance of diarylethene switches," J. Am. Chem. Soc. **137**, 2738–2747 (2015).
39. M. Irie, T. Lifka, K. Uchida, S. Kobatake, and Y. Shindo, "Fatigue resistant properties of photochromic dithienylethenes: by-product formation," Chem. Commun. **8**, 747–750 (1999).
40. S. Fredrich, R. Göstl, M. Herder, L. Grubert, and S. Hecht, "Switching diarylethenes reliably in both directions with visible light," Angew. Chem. Int. Ed. **55**, 1208–1212 (2016).
41. D. Mendive-Tapia, A. Perrier, M. J. Bearpark, M. A. Robb, B. Lasorne, and D. Jacquemin, "New insights into the by-product fatigue mechanism of the photo-induced ring-opening in diarylethenes," Phys. Chem. Chem. Phys. **16**, 18463–18471 (2014).
42. G. Pariani, M. Quintavalla, L. Colella, L. Oggioni, R. Castagna, F. Ortica, C. Bertarelli, and A. Bianco, "New insight into the fatigue resistance of photochromic 1, 2-diarylethenes," J. Phys. Chem. C **121**, 23592–23598 (2017).
43. E. Samoylova, W. Dallari, M. Allione, F. Pignatelli, L. Marini, R. Cingolani, A. Diaspro, and A. Athanassiou, "Characterization of fatigue resistance in photochromic composite materials for 3D rewritable optical memory applications," Mater. Sci. Eng. B **178**, 730–735 (2013).
44. D. Cambié, J. Dobbelaar, P. Riente, J. Vanderspikken, C. Shen, P. H. Seeberger, K. Gilmore, M. G. Debije, and T. Noël, "Energy-efficient solar photochemistry with luminescent solar concentrator based photomicroreactors," Angew. Chem. Int. Ed. Engl. **58**, 14374–14378 (2019).